



# Magnesium-doped calcium phosphate/sodium alginate biocomposite for bone implant application

Sharifah Adzila<sup>1</sup> · Nor Azimah Mustaffa<sup>1</sup> · Nanthini Kanasan<sup>1</sup>

Received: 8 October 2018 / Revised: 29 August 2019 / Accepted: 23 October 2019 / Published online: 2 January 2020  
© Australian Ceramic Society 2020

## Abstract

Calcium phosphate (CaP) is well known as biocompatible and bioactive materials that helps in bone growth. However, the brittleness of CaP makes it limited in load-bearing application. The effect of magnesium (Mg) doping in various weight percentages on the physical and mechanical properties of CaP/sodium alginate (SA) biocomposite was investigated. Mg-doped CaP/SA biocomposite powder was prepared by using precipitation method. 95/5 ratio of CaP/SA was used to be doped with different weight percentages (wt%) of Mg. The maximum hardness was attained at 5.34 GPa for 1.5 wt% of Mg-doped CaP/SA. The maximum grain size of 3.75  $\mu\text{m}$  at 1.0 wt% of Mg-doped CaP/SA was observed under scanning electron microscope (SEM) micrograph which also represents the maximum density of 2.91  $\text{g}/\text{cm}^3$ . Characterization of Mg-doped CaP/SA powder through Fourier-transform infrared (FTIR) exhibited the phosphate ( $\text{PO}_4$ ) group was reduced with the increase of Mg doping which was also supported in X-ray diffraction (XRD) analysis. From the analyses, Mg ion doping improves the properties of CaP/SA biocomposite.

**Keywords** Calcium phosphate · Sodium alginate · Magnesium · Biocomposite · Bone implant

## Introduction

The similarity of calcium phosphate (CaP) to the natural bone makes it being used in bone substitution or implantation [1]. Human bone consist of 70% of minerals that include calcium (39%), phosphate (17%), sodium (0.7%), magnesium (0.5%), and others (0.7%) [2]. CaP is well known as biocompatible and bioactive materials that helps in bone growth [2]. Apatite formation that observed in both in vivo and in vitro tests in CaP sample [3] was confirmed in the biocompatibility and bioactivity of the material [4]. However, the brittleness of CaP [5] makes it limited in load-bearing application. Due to that, a lot of methods like composite [6, 7], doping [8, 9], coating [10, 11], etc. has been used to improve the strength of the CaP. The

resorbability was depending on the ratio and structure of CaP where hydroxyapatite (HA) was described as “nonresorbable” and tricalcium phosphate (TCP) as “resorbable.” Resorbability of the material was described as degradation of material in vivo [12]. Since the SA is one of material with high biodegradation rate which can improved the properties of CaP, SA is also known as biocompatible, hydrophilic material, and it is widely used in biomedical application as wound dressing [13, 14], drug delivery [15], and tissue engineering [16]. SA provides a good addition in HA since it shows increasing in the hardness as well as in density of HA [6, 7]. Mg was used in doping process since it promotes new bone growth [17]. Furthermore, human body needs a number of metals (ions) for normal physiological functioning such as sodium ( $\text{Na}^+$ ), magnesium ( $\text{Mg}^{2+}$ ), etc. [18]. The Mg found as a material that safe degrade in human body and replace by a new bone but the release can be toxic if Mg is too high in human body [19]. Doping the Mg into CaP-based ceramic has shown good biocompatibility without any cytotoxicity effect [20, 21]. In this study, the CaP already mixed with sodium alginate (SA) as composite material. Among the ratio of CaP/SA that had been done, 95/5 ratio was found in the

✉ Sharifah Adzila  
adzila@uthm.edu.my

<sup>1</sup> Faculty of Mechanical & Manufacturing Engineering, Universiti Tun Hussein Onn Malaysia, 86400 Batu Pahat, Johor, Malaysia

highest hardness and density properties. The ratio was then doped with different weight percentage (1.0 to 2.0 wt%) of magnesium (Mg) to discover the effect of Mg in properties of CaP/SA.

## Experimental

### Material preparation

Calcium phosphate powder, CaP ( $\text{CaHPO}_4$ ), was commercially available from Fisher Chemical, Fisher Scientific, Sodium Alginate powder, SA ( $\text{NaC}_6\text{H}_7\text{O}$ ) from R&M Chemicals and Magnesium Hydroxide powder, and Mg ( $\text{MgOH}_2$ ) from Q-Rec. Mg-doped CaP/SA were prepared by using a precipitation method with different weight percentage of Mg (1.0–2.0 wt%). CaP and SA powders with 95/5 ratio were mixed first and then doped with Mg. The process was started by stirring the CaP powder with distilled water at 80 °C for 2 h. Then, SA was slowly added into the mixture and leaved it for another 2 h. Mg was doped into CaP/SA by using similar preparation. The precipitated powder was aged for 24 h at room temperature before oven dried at 80 °C. Then, the dried powders were crushed and compacted uniaxially under 2-tonne (9.19 MPa) pressures. The samples were then sintered in air at 1000 °C at 2 °C/min heating for 2 h.

### Characterization

FTIR measurement was carried out by using Perkin Elmer. The prepared powders were recorded in the region between 530 and 4000  $\text{cm}^{-1}$  with 4  $\text{cm}^{-1}$  spectral resolution, and 32 scan number. XRD was performed on prepared and sintered powders. The analysis was set at 40 kV and 40 mA with diffraction angles ( $2\theta$ ) between 25° and 55° with step size of 0.02° per second. The physical property of the samples was determined via bulk density. Bulk density of the sample was measured by using Archimedes' theory by Mettler Toledo Density kit. The dry weight (Wd), immersed weight (Ws), and wet weight (Ww) of samples were recorded, and the density of water ( $\rho_{\text{water}}$ ) is taken as 1.0  $\text{g}/\text{cm}^3$ . The samples surface were grinded and polished prior to Vickers hardness test. Ten indentations under load Hv 0.2 (1.961 N) were taken in every sample. In order to reveal the microstructure, heat treatment was conducted under atmospheric furnace with 950 °C with 2 °C/min heating rate. Since CaP is ceramic material, the sample was coated with platinum to prevent charging phenomenon occurred. Based on the SEM micrograph image,

the average grain size was calculated by using line intercept method (ASTM E 112-96, 2004).

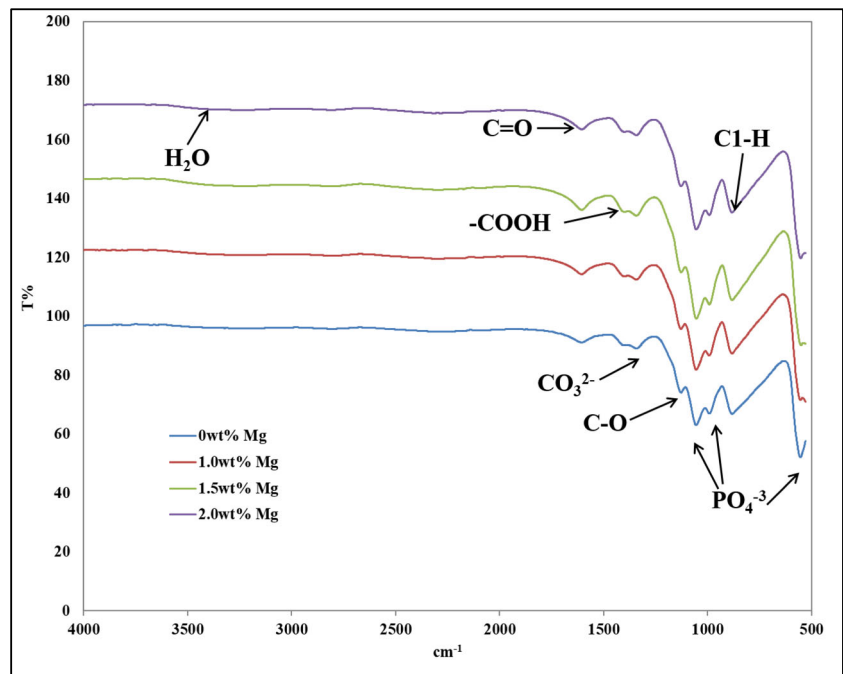
## Results and discussion

### Characterization

Figures 1 and 2 show the FTIR analysis at different weight % of Mg-doped CaP/SA. It is clearly showed that the phosphate group ( $\text{PO}_4^{-3}$ ) existence was remain at a range from 976  $\text{cm}^{-1}$ –1190  $\text{cm}^{-1}$  and 520  $\text{cm}^{-1}$ –600  $\text{cm}^{-1}$  before and after sintering [22, 23]. The bands' intensity was reduced with Mg doping which indicates the replacement of Mg ion and has led to the decreasing of Ca/P ratio [24]. The alginate functional groups were disappeared after sintering which referred to the carboxyl (C = O) stretching vibration (1590  $\text{cm}^{-1}$  to 1750  $\text{cm}^{-1}$ ) and carboxyl-COOH stretching band (1405  $\text{cm}^{-1}$  to 1456  $\text{cm}^{-1}$ ) [25]. Hence, before sintering, these bands were also decreased with the increase of Mg ion doping. However, Only C-O stretching vibration (1020.9  $\text{cm}^{-1}$  to 1027.8  $\text{cm}^{-1}$ ) [25] was detected after the sintering and doping processes.  $\text{H}_2\text{O}$  is also one of the band that losses after the sintering process since the water was released during the sintering process. The new peaks were observed after sintering process that belong to the  $\text{P}_2\text{O}_7^{4-}$  and  $\text{SO}_4^{2-}$  bands which assigned at 1200  $\text{cm}^{-1}$  and 720  $\text{cm}^{-1}$  and 1160  $\text{cm}^{-1}$  and 1140  $\text{cm}^{-1}$ , respectively. The intensity of the  $\text{P}_2\text{O}_7^{4-}$  and  $\text{SO}_4^{2-}$  bands were decreased with the increase of  $\text{Mg}^{2+}$  in CaP.  $\text{P}_2\text{O}_7^{4-}$  band is also known as  $\beta$ -TCP which existed when heat treatment has been applied at 800 °C to 1000 °C [26]. The formation of  $\beta$ -TCP also can be observed in XRD analysis (Figs. 3 and 4) where  $\beta$ - $\text{Ca}_3(\text{PO}_4)_2$  phase was existed after sintering process.

XRD analyses of Mg-doped CaP/SA at different weight percentages are shown in Figs. 3 and 4. Based on the figures, the formation of the Mg-whitlockite after doping was observed before and after the sintering process. However, different phase was observed with different condition where the Mg-whitlockite ( $\text{Ca}_{18}\text{Mg}_2\text{H}_2(\text{PO}_4)_{14}$ ) was referred before the sintering process. Meanwhile, the Mg-whitlockite with ( $\text{Ca}_{2.71}\text{Mg}_{0.29}(\text{PO}_4)_2$ ) was observed after the sintering process where this might due to the changing crystal structure in sample when heat was applied [27]. The intensities of both phases were increased with increasing of Mg. Another phase that observed after the sintering process is CaP-whitlockite ( $\text{Ca}_3(\text{PO}_4)_2$ ) which was only observed in undoped CaP/SA. The phase was disappeared and replaced with Mg-whitlockite ( $\text{Ca}_{2.71}\text{Mg}_{0.29}(\text{PO}_4)_2$ ) after doping with Mg ion. This change has proved the

**Fig. 1** FTIR analysis on prepared powder at different wt% of Mg-doped CaP/SA



substitution of Mg in CaP/SA.  $\text{Ca}_2\text{P}_2\text{O}_7$  peak decreased with the addition of Mg ion due to the substitution of Mg in CaP/SA. This is in line with Zhengsheng et. al., (2005) [24] where the substitution of Mg occurred which lead to the decrease of HA intensity peak.

**Density and hardness**

The density and hardness at different wt% of Mg-doped CaP/SA are shown in Figs. 5 and 6, respectively. The

graphs clearly showed that the addition of Mg ion increased the density and hardness of CaP/SA. Figure 5 shows the density sharply increased from undoped CaP/SA at  $2.13 \text{ g/cm}^3$  to the maximum density at 1 wt% of Mg-doped CaP/SA with  $2.93 \text{ g/cm}^3$ . The density starts to decrease at 1.5 wt% of Mg-doped CaP/SA. Figure 6 shows the hardness increase linearly from undoped CaP/SA to 1.5 wt% of Mg-doped CaP/SA and drop at 2.0 wt% of Mg-doped CaP/SA. The maximum hardness was obtained at 5.39 GPa at 1.5 wt% of Mg-doped CaP/SA, and the

**Fig. 2** FTIR analysis of Mg-doped CaP/SA at different wt% sintered at 1000 °C

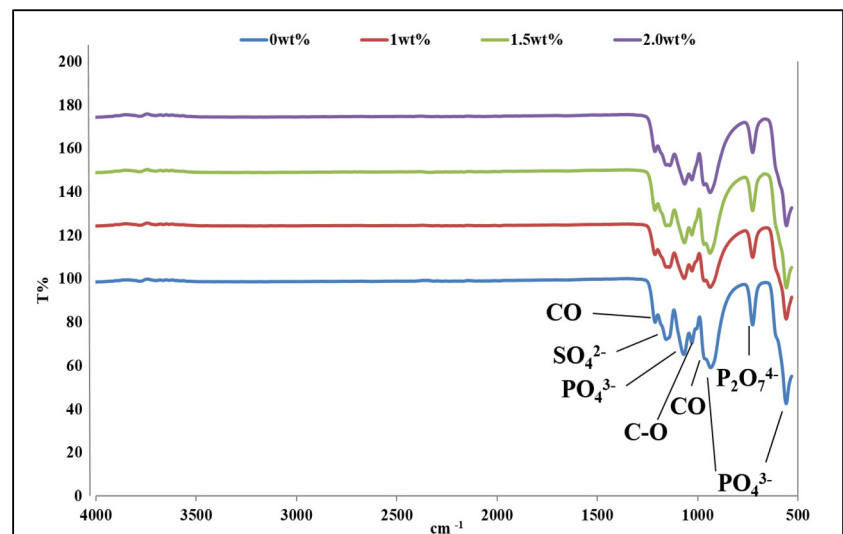
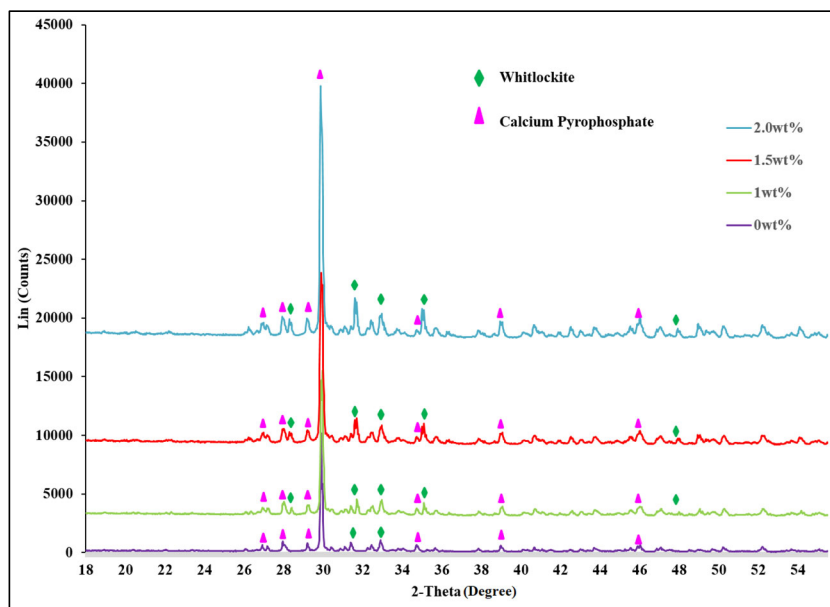


**Fig. 3** XRD analysis on synthesized powder of different wt% of Mg-doped CaP/SA



minimum hardness was observed in undoped CaP/SA with 4.70 GPa. Based on the figures, the hardness was not averagely affected by the density, but it is directly influenced by the grain size [8].

### SEM analysis

Figures 7 and 8 show the SEM micrograph and average grain size of undoped CaP/SA and Mg-doped CaP/SA at

different weight percentage, respectively. Figure 7 clearly shows that the undoped CaP/SA contained more porosities than Mg-doped CaP/SA, and the grain size that becomes larger with the addition of Mg ion indicates that Mg doping provides significant impact to the grain size and porosity of CaP/SA. All the samples show an equiaxed shapes. The average grain size in Fig. 8 shows the similar trend with the SEM micrograph where the presence of  $Mg^{2+}$  increased the average grain size of

**Fig. 4** XRD analysis on different weight % Mg-doped CaP/SA sintered at 1000 °C

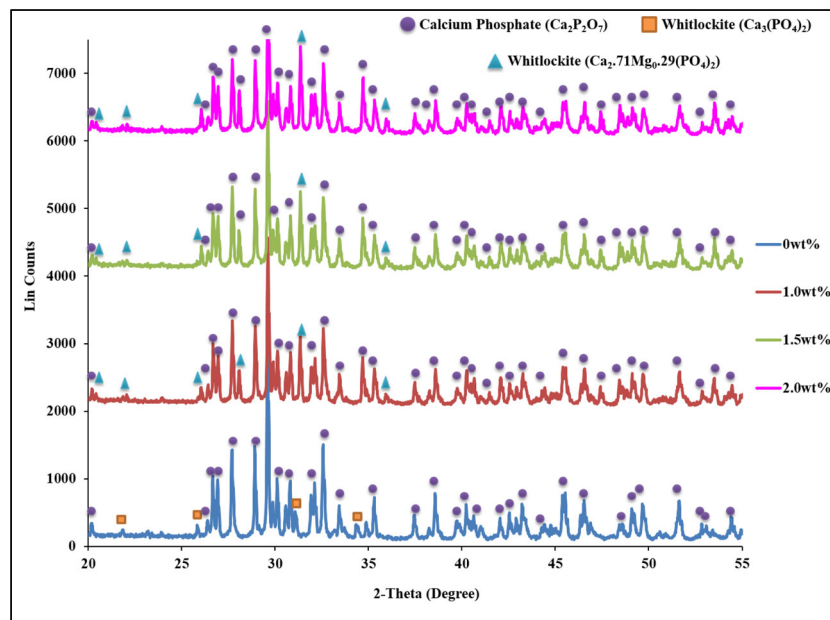
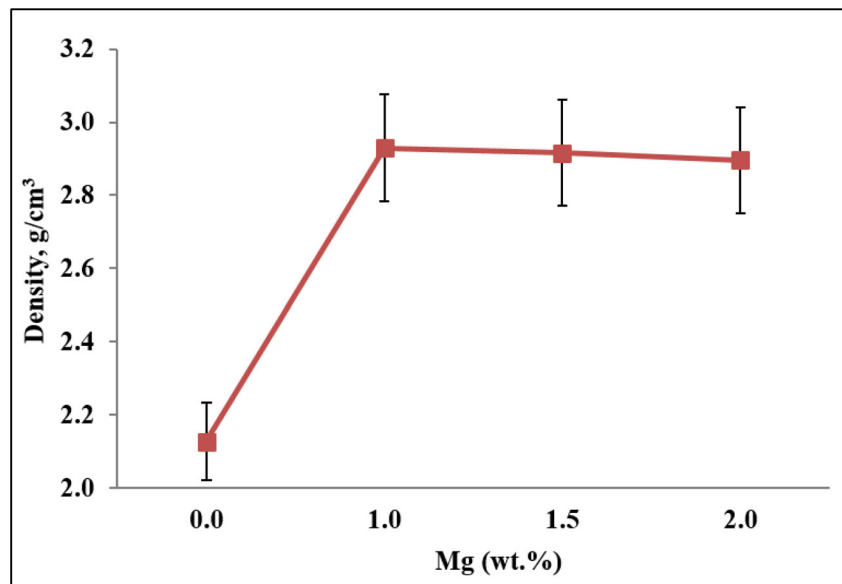


**Fig. 5** Density at different weight % of Mg-doped CaP/SA



CaP/SA. The minimum grain size was obtained in undoped CaP/SA with 1.59 μm where it relates to the minimum density and hardness which affected by the small grains and high porosities. The maximum average grain size was exhibited at 1.0 wt% of Mg-doped CaP/SA with 3.75 μm which also relates to the maximum density where the grain growth reduced the porosity. However, the maximum hardness was not obtained at 1.0 wt% of Mg-doped CaP/SA even it shows larger grain size. Previous studies reported that the existence of close porosity and large grain size was led to the decreasing of

hardness [8, 27]. In this study, the maximum hardness obtained at 1.5 wt% of Mg-doped CaP/SA shows the combination of large and small grains with 2.61 μm average grain size. According to Adzila et al. (2016) [8], the combination of large and small grain has led to the strong bonding among the grains which increased the hardness of the sample. The density and hardness obtained from Adzila et. al. (2016) [8] in Mg-doped HA were at 3.46 g/cm<sup>3</sup> and 1.13GPa, respectively, at 1100 °C. However, the hardness at 1000 °C obtained in this present study was higher compared to Adzila et al. (2016) [8] that might due

**Fig. 6** Hardness at different weight % of Mg-doped CaP/SA

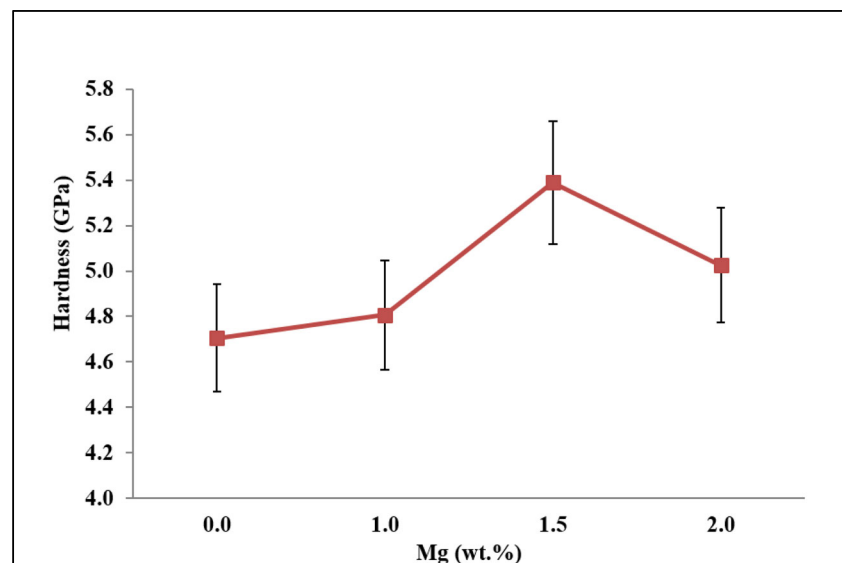
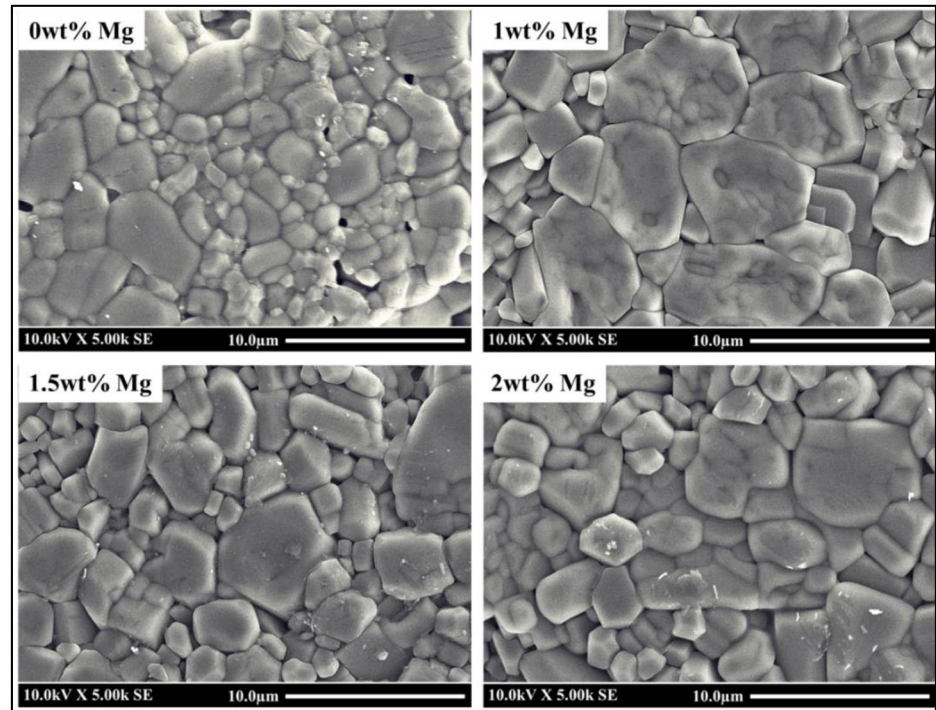


**Fig. 7** Microstructure of undoped CaP/SA and Mg-doped CaP/SA at different weight percentages



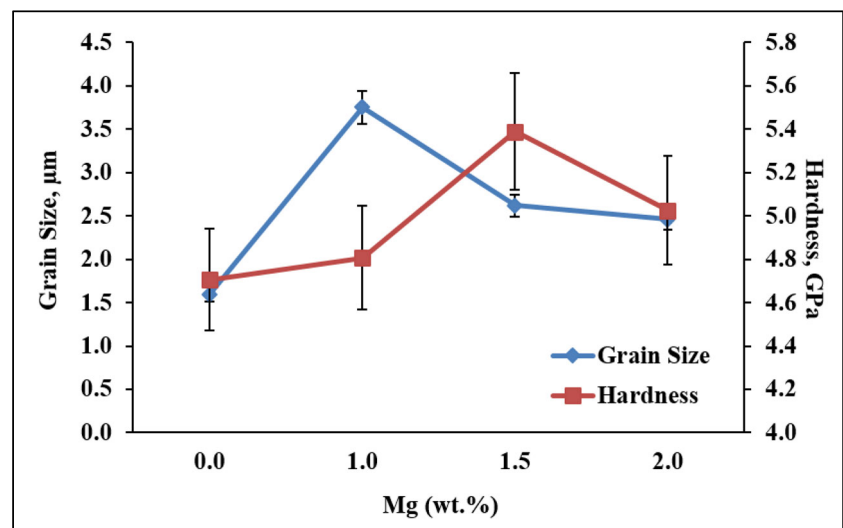
to the addition of SA. In this present study, the grain size is one of the factors influenced in density and hardness of the Mg-doped CaP/SA biocomposite.

## Conclusion

Mg-doped CaP/SA at various weight percentages have been successfully prepared by using precipitation method which

has been proved in FTIR and XRD analyses. The presence of the Mg in CaP/SA biocomposite has shown significant effects in density and hardness with maximum value obtained at 2.91 g/cm<sup>3</sup> and 5.34 GPa, respectively, at 1 wt% to 1.5 wt% Mg. The improvement in hardness and density was directly influenced by the grain size. The combination of large and small grains has led to the strong bonding formation between the grains which increased the hardness. The improvement in physical and mechanical properties can contribute the Mg-

**Fig. 8** Comparison of the average grain size and hardness of undoped CaP/SA and Mg-doped CaP/SA at different weight percentages



doped CaP/SA in bone implant application specifically in load-bearing condition.

**Acknowledgments** This study was supported by GPPS Grant No. U472 and Contract Grant No. U562 from Research Management Centre (RMC), Universiti Tun Hussein Onn Malaysia (UTHM).

## References

- Ghosal, S.: Densification and mechanical characterization of pure and doped hydroxyapatite. Thesis, National Institute of Technology, Rourkela. <http://ethesis.nitrkl.ac.in/4791/1/109CR0110.pdf> (2013). Accessed June 2017.
- Roemhildt, M. L.: Calcium phosphate compatible bone cement : characterization, bonding properties and tissue response. Thesis, Iowa State University. <https://lib.dr.iastate.edu/cgi/viewcontent> (2002). Accessed June 2017.
- Xin, R., Leng, Y., Chen, J., Zhang, Q.: A comparative study of calcium phosphate formation on bioceramics in vitro and in vivo. *Biomaterials*. **26**, 6477–6486 (2005)
- Karatas, O.: Investigation of biocompatibility of calcium phosphate based materials and cements. DSpace@IZTECH Web. <http://hdl.handle.net/11147/4172> (2014). Accessed 18 Nov 2017.
- Ambard, A.J., Mueninghoff, L.: Calcium phosphate cement : review of mechanical and biological properties. *J. Prosthodont*. **15**, 321–328 (2006)
- Rajkumar, M., Meenakshisundaram, N., Rajendran, V.: Development of nanocomposites based on hydroxyapatite/sodium alginate: synthesis and characterisation. *Mater. Charact*. **62**, 469–479 (2011)
- Kanasan, N., Adzila, S., Azimah Mustaffa, N.: The effect of sodium alginate on the properties of hydroxyapatite. *Procedia Eng*. **184**, 442–448 (2017)
- Adzila, S., Kanasan, N., Hassan, M.F., Mubarak, A., Yunus, M.Z., Rahman, M.N.A., Haq, R.: Synthesis and characterization of magnesium doped calcium phosphate for bone implant application. *ARPN J. Eng. Appl. S ci*. **11**, 8694–8697 (2016)
- Tan, C.Y., Yaghoubi, A., Ramesh, S., Adzila, S., Purbolaksono, J.: Sintering and mechanical properties of MgO-doped nanocrystalline hydroxyapatite. *Ceram. Int*. **39**, 8979–8983 (2013)
- Habibovic, P.F., Barre, C., Van Blitterswijk, A., De Groot, K.: Biomimetic hydroxyapatite coating on metal implants. *J. Am. Ceram. Soc*. **85**, 517–522 (2002)
- Mohseni, E., Zalnezhad, E., Bushroa, A.R.: Comparative investigation on the adhesion of hydroxyapatite coating on Ti– 6Al– 4 V Implant: A Review Paper. *Int. J. Adhes. Adhes*. **48**, 238–257 (2014)
- Al-sanabani, J.S., Madfa, A.A., Al-sanabani, F.A.: Application of calcium phosphate materials in dentistry. *Int. J. Biomaterials*. **2013**(12), (2013)
- Kim, H., Lee, H., Oh, J., Shin, B.A., Oh, C.S., Park, R.D., Yang, K.S., Cho, C.S.: Polyelectrolyte complex composed of chitosan and sodium alginate for wound dressing application. *Aust. J. Biol. Sci*. **543–556** (1999)
- Paul, W., Sharma, C.P.: Chitosan and alginate wound dressings: a short review. *Trends Biomater. Artif. Organs*. **18**, 17–23 (2015)
- Tønnesen, H.H., Karlsen, J.: Alginate in drug delivery systems. *Drug Dev. Ind. Pharm*. **28**, 621–630 (2002)
- Lin, H. R., Yeh, Y. J.: Porous Alginate / Hydroxyapatite Composite Scaffolds for Bone Tissue Engineering: Preparation , Characterization , and In Vitro Studies. *J Biomed. Mater. Res. B Appl. Biomater*. **71**(1), 52–65 (2004)
- Witte, F.: Acta Biomaterialia Reprint of : The history of biodegradable magnesium implants : a review. *Acta Biomater*. **23**, 528–540 (2009)
- Kirkland, N.T.: Magnesium biomaterials-past, present and future. *J. Chem. Inf. Model*. **53**, 160 (2012)
- Ryu, H., Sun, K., Lee, J., Joong, D., Hyup, J., Chang, B., Lee, D., Lee, C., Chung, S.: Magnesia-doped HA/ $\beta$ -TCP ceramics and evaluation of their biocompatibility. *Biomaterials*. **25**, 393–401 (2004)
- Ryu, H., Youn, H., Sun, K., Chang, B.: An improvement in sintering property of  $\beta$ -tricalcium phosphate by addition of calcium pyrophosphate. *Biomaterials*. **23**, 909–914 (2002)
- Rehman, I., Bonfield, W.: Characterization of hydroxyapatite and carbonated apatite by photo acoustic FTIR spectroscopy. *J. Mater. Sci. Mater. Med*. **8**, 1–4 (1997)
- Slosarczyk, A., Paszkiewicz, Z., Paluszkiwicz, C.: FTIR and XRD evaluation of carbonated hydroxyapatite powders synthesized by Wet Methods. *J. Mol. Struct*. **747**, 657–661 (2005)
- Adzila, S., Ramesh, S., Sopyan, I., Tan, C.Y., Hamdi, M., Teng, W.D.: Mechanochemical synthesis of magnesium doped hydroxyapatite : powder characterization. *Appl. Mech. Mater*. **372**, 62–65 (2013)
- Zhensheng, L., Ramay, H.R., Hauch, K.D., Xiao, D., Zhang, M.: Chitosan-alginate hybrid scaffolds for bone tissue engineering. *Biomaterials*. **26**, 3919–3928 (2005)
- Berzina-cimdina, L., Borodajenko, N.: Research of Calcium Phosphates Using Fourier Transform Infrared Spectroscopy. IntechOpen Web. <https://www.intechopen.com/books/infrared-spectroscopy-materialscience-engineering-and-technology/research-of-calcium-phosphates-using-fourier-transformation-infraredspectroscopy> (2012). Accessed 10 May 2017.
- Osborn, J.F.: The material science of calcium phosphate ceramics. *Biomaterial*. **1**, 108–111 (1980)
- Thangamani, N., Chinnakali, K., Gnanam, F.D.: The effect of powder processing on densification, microstructure and mechanical properties of hydroxyapatite. *Ceram. Int*. **28**, 355–362 (2002)

**Publisher's note** Springer Nature remains neutral with regard to jurisdictional claims in published maps and institutional affiliations.